Sound Source Radiation in Two-Dimensional Shear Flow

Sébastien M. Candel*
Office National d'Etudes et de Recherches Aérospatiales, Châtillon, France

A fundamental problem encountered in the analysis of aerodynamic noise is that of acoustic source radiation in nonhomogeneous flow. Exact numerical solutions have been obtained recently for source radiation near a plane interface and a shear discontinuity by directly synthesizing the wavefield from its spatial Fourier transform. This method is applied here to stratified flow configurations and the structure of the radiated field is obtained for several shear layer velocity profiles of practical interest.

Nomenclature

$A_j(\alpha), B_j(\alpha)$ = amplitudes of outgoing and incoming waves in layer j
c = sound speed
d = layer thickness
i = complex number, $\sqrt{-1}$
k = wavenumber
ℓ = spatial extension of the calculation domain
L = layer index corresponding to a selected value of attenuation
M = Mach number
N = number of points in the discrete Fourier transform
p = pressure
$\tilde{p}$ = Fourier transform of pressure
Q = total number of shear discontinuities used to represent the flow
S = cumulated transfer matrix
T = layer transfer matrix
U = mean flow velocity
x,z = Cartesian coordinates
α = spatial wavenumber, argument of Fourier transform
$\alpha_{j\pm}$ = branch points of γ_j
γ_j = phase or damping factor for waves in layer j
$\delta(\ )$ = delta function
Δx = spatial sampling period
$\Delta\alpha$ = spatial wavenumber sampling period
η = interfacial displacement
Θ = polar angle measured with respect to the x axis
λ = wavelength
ω = angular frequency

Subscripts

$*$ = reduced (dimensionless) quantity
j = layer index

I. Introduction

A FUNDAMENTAL problem encountered in the analysis of aerodynamic noise is that of acoustic source radiation in nonhomogeneous flow. In the general case where the flowfield is three dimensional or when the sound source is situated off the symmetry axis of the flow, the radiated wavefield may be calculated effectively by making use of standard approximations. One suitable method for these complicated problems is based on the geometrical approximation. It is, indeed, possible to obtain a complete numerical implementation of the first-order geometric solution for the most general flow case.[1]

This numerical technique has been used extensively by us to analyze sound source radiation from jets, refraction effects in open wind tunnels, shielding by fluid screens, and wave motion in nozzles.[2] The geometric technique is powerful, but due to its approximate nature, it cannot account for wave diffraction in the domain of propagation. When refraction and diffraction occur simultaneously it is more appropriate to base the calculation on the parabolic approximation. This method is well suited to the treatment of weakly inhomogeneous cases such as those encountered in scattering problems.[3] Now, in many practical situations one is interested in acoustic fields of low or intermediate frequencies propagating in strongly nonhomogeneous flows. While the general three-dimensional problems of this type cannot be solved without resorting to finite difference or finite element computations, it is much easier to deal with shear flow situations. For such cases exact numerical solutions may be determined by directly synthesizing the wavefield from its spatial Fourier transform. This spectral method was recently used to investigate sound source radiation near a plane interface[4] and near a shear discontinuity.[5] It is applied here to source radiation in stratified shear flow configurations.

While this problem does not correspond to any practical situation, it has been used extensively to model noise radiation from free jets.[6-9] A good synthesis of the results obtained in these studies is presented by Goldstein.[10] Further investigations have been carried out by Scott[11] and Koutsoyanis et al.[12] Other studies pertinent to this problem are those of Refs. 13-17.

In distinction with these previous studies our treatment is essentially numerical and does not rely on approximation techniques such as the method of steepest descent or the method of stationary phase. Furthermore, most previous studies assumed linear shear layer profiles. This assumption simplifies analytical work but there is a loss of generality. There is no such restriction in the present work.

The only simplifications used here are to 1) consider line source radiation and 2) describe the shear layer profile by an ensemble of adjacent plug flows of constant properties. The first assumption is not fundamental and the method presented is equally suited to the treatment of point source radiation in axisymmetric configurations. The second assumption is consistent with our numerical approach. Indeed, a continuous shear layer profile may be represented to any degree of accuracy by a staircase function by increasing the number of layers used in the calculation. The main advantage of this procedure is that it replaces numerical integration of ordinary

Presented as Paper 81-2042 at the AIAA 7th Aeroacoustics Meeting, Palo Alto, Calif., Oct. 3-5, 1981; submitted Oct. 16, 1981; revision received April 17, 1982.

*Visiting Research Scholar, Joint Institute for Aeronautics and Acoustics, Stanford University, Stanford, Calif.; Research Scientist and Professor of Engineering at Ecole Centrale des Arts et Manufactures, Chatenay-Malabry, France. Member AIAA.

differential equations by matrix multiplications thus bringing a considerable reduction of computer time. To be rigorous it is necessary to show that the solution obtained under this second assumption indeed converges to a limit when the number of layers is increased and that this limit coincides with the wave-like solution of the propagation problem in a continuous mean flow. A proof of this point may be based on a discussion presented by Goldstein[10] (pp. 10-22) in an analysis of wavemotion in a region of mean flow velocity adjustment. According to Goldstein, when the thickness δ of the adjustment region is much smaller than the wavelength λ it is possible to replace the velocity profile by a fictitious velocity discontinuity which a) sustains no force in the transverse direction and b) follows the local fluid motion. In other words, the pressure and transverse displacement must be continuous across the shear discontinuity representing the velocity adjustment. Now, any finite shear region may be subdivided in a number of layers of velocity adjustment characterized by a thickness $\delta \ll \lambda$. Then, each thin layer may be replaced by an equivalent shear discontinuity. The solution obtained with this plug flow model then converges toward a wave-like solution of the continuous problem when the number of layers is increased. It is, however, essential to ensure continuity of pressure and displacement across each interface, two conditions introduced by Miles[18] and Ribner[19] in their pioneering analysis of plane waves impinging on a shear discontinuity.

Analytical development of our method is briefly carried in Sec. II. Practical details on discretization and Fourier synthesis are provided in Sec. III. Section IV describes various examples of calculation.

II. Analytic Development

The present analysis follows classical methods and only a brief description is required. We confine our attention to the flow model of Fig. 1. A line source S of amplitude 4π is located at $x=z=0$ in a parallel shear flow. The flow Mach number and sound speed are only function of the z coordinate $M=M(z)$, $c=c(z)$. The source is monochromatic and all waves have a common factor $\exp(-i\omega t)$.

Now, the continuous profile of Fig. 1a may be replaced by a staircase function by dividing the shear region in $Q+1$ plug flows (Fig. 1b). Each layer is characterized by its index j, Mach number M_j, sound speed c_j, and transverse dimension d_j. The lower and upper interfaces bounding the jth layer are located at $z=z_j$ and $z=z_{j+1}$, respectively.

The pressure field in each layer satisfies a convected wave equation

$$(1-M_j^2)\frac{\partial^2 p_j}{\partial x^2}+\frac{\partial^2 p_j}{\partial z^2}+2ik_jM_j\frac{\partial p_j}{\partial x}+k_j^2 p=-4\pi\delta(x)\delta(z) \tag{1}$$

where $k_j=\omega/c_j$.

The source term appearing on the right-hand side of this equation vanishes identically except in the first layer.

Matching conditions at each interface are those obtained by specifying that pressure and displacement are continuous functions (the conditions of Miles[18] and Ribner[19]). On the $z=z_{j+1}$ interface these conditions have the form

$$p_j(x,z_{j+1})=p_{j+1}(x,z_{j+1}),\quad \eta_j(x,z_{j+1})=\eta_{j+1}(x,z_{j+1}) \tag{2}$$

The local displacement η is obtained from the pressure by making use of the linearized momentum equation

$$\rho_j c_j^2\left(-ik_j+M_j\frac{\partial}{\partial x}\right)^2\eta_j=-\frac{\partial p_j}{\partial z} \tag{3}$$

$$\rho_{j+1}c_{j+1}^2\left(-ik_{j+1}+M_{j+1}\frac{\partial}{\partial x}\right)^2\eta_{j+1}=-\frac{\partial p_{j+1}}{\partial z} \tag{4}$$

In addition to the previous relations, it is necessary to impose radiation conditions in the first and last layers.

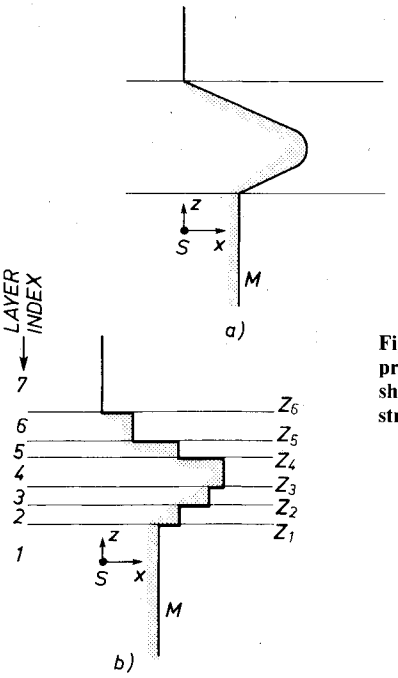

Fig. 1 Geometry of the problem: a) continuous shear layer profile and b) stratified representation.

The problem just defined may be formally solved by transformation methods. Let $\tilde{p}_j(\alpha,z)$ and $\tilde{\eta}_j(\alpha,z)$ designate the Fourier transforms of pressure and displacement in the jth layer

$$p_j(x,z)=\int\tilde{p}_j(\alpha,z)e^{i\alpha x}\mathrm{d}\alpha \qquad j=1,2,\ldots,Q+1 \tag{5}$$

$$\eta_j(x,z)=\int\tilde{\eta}_j(\alpha,z)e^{i\alpha x}\mathrm{d}\alpha \qquad j=1,2,\ldots,Q+1 \tag{6}$$

then, the transformed wave equation and matching conditions take the form

$$\frac{\mathrm{d}^2\tilde{p}_j}{\mathrm{d}z^2}-\gamma_j^2\tilde{p}_j=-2\delta(z) \tag{7}$$

$$\tilde{p}_j(\alpha,z_{j+1})=\tilde{p}_{j+1}(\alpha,z_{j+1}) \tag{8}$$

$$\begin{aligned}\tilde{\eta}_j(\alpha,z_{j+1})&=\frac{1}{\rho_j c_j^2\delta_j^2}\frac{\mathrm{d}\tilde{p}_j}{\mathrm{d}z}(\alpha,z_{j+1})\\&=\frac{1}{\rho_{j+1}c_{j+1}^2\delta_{j+1}^2}\frac{\mathrm{d}\tilde{p}_{j+1}}{\mathrm{d}z}(\alpha,z_{j+1})\\&=\tilde{\eta}_{j+1}(\alpha,z_{j+1})\end{aligned} \tag{9}$$

where $\gamma_j=[(1-M_j^2)\alpha^2+2M_jk_j\alpha-k_j^2]^{1/2}$ and $\delta_j=k_j-M_j\alpha$.

The γ_j possess two branch points $\alpha_{j+}=k_j/(1+M_j)$ and $\alpha_{j-}=-k_j/(1-M_j)$ and it is necessary to select a unique determination of these factors. The choice must be consistent with the radiation conditions at infinity. Standard considerations (see, for example, Ref. 5) lead to the following definitions.

Let

$$\nu_j=|(1-M_j^2)\alpha^2+2M_jk_j\alpha-k_j^2|^{1/2}$$

then, for a subsonic medium we take $\gamma_j=\nu_j$ for $\alpha<\alpha_{j-}$ or $\alpha>\alpha_{j+}$ and $\gamma_j=-i\nu_j$ for $\alpha_{j-}\le\alpha\le\alpha_{j+}$. Here, γ_j acts as a phase factor when the spatial wavenumber α belongs to $[\alpha_{j-},\alpha_{j+}]$ and as a damping factor outside this interval. Note that it is physically significant that damping occurs when the spatial plane wave $\tilde{p}_j$ (the spatial Fourier component) propagates at an angle Θ less than $\cos^{-1}[1/(1+M_j)]$. For a supersonic medium the proper determination is $\gamma_j=\nu_j$ for

$\alpha_{j+} \leq \alpha \leq \alpha_{j-}$, $\gamma_j = i\nu_j$ for $\alpha_{j-} < \alpha$, and $\gamma_j = -i\nu_j$ for $\alpha < \alpha_{j+}$. In this situation γ_j is a damping factor when α belongs to $[\alpha_{j+}, \alpha_{j-}]$ and behaves like a phase factor outside this interval.

Now, the general solution of Eq. (7) has the form

$$\tilde{p}_j(\alpha,z) = A_j(\alpha)e^{-\gamma_j(z-z_j)} + B_j(\alpha)e^{\gamma_j(z-z_j)} \tag{10}$$

where $A_j(\alpha)$ and $B_j(\alpha)$ are yet to be determined. Direct application of the transformed matching conditions leads to the following relations.

$$A_j e^{-\gamma_j d_j} + B_j e^{\gamma_j d_j} = A_{j+1} + B_{j+1} \tag{11}$$

$$A_j e^{-\gamma_j d_j} - B_j e^{\gamma_j d_j} = \mu_j [A_{j+1} - B_{j+1}] \tag{12}$$

where

$$\mu_j = (\rho_j c_j^2 \delta_j^2 / \rho_{j+1} c_{j+1}^2 \delta_{j+1}^2)(\gamma_{j+1}/\gamma_j)$$

Thus, the transformed field amplitudes A_j, B_j are related to A_{j+1}, B_{j+1} by a transfer matrix

$$\begin{bmatrix} A_j \\ B_j \end{bmatrix} = T_j \begin{bmatrix} A_{j+1} \\ B_{j+1} \end{bmatrix} \tag{13}$$

with

$$T_j = \frac{1}{2}\begin{bmatrix} (1+\mu_j)e^{\gamma_j d_j} & (1-\mu_j)e^{\gamma_j d_j} \\ (1-\mu_j)e^{-\gamma_j d_j} & (1+\mu_j)e^{-\gamma_j d_j} \end{bmatrix} \tag{14}$$

It is then possible to express the field amplitudes in the first layer in terms of those existing in the last layer.

$$\begin{bmatrix} A_1 \\ B_1 \end{bmatrix} = S(1,Q) \begin{bmatrix} A_{Q+1} \\ B_{Q+1} \end{bmatrix} \tag{15}$$

where $S(1,Q) = T_1 T_2 \ldots T_Q$ designates the cumulated transfer matrix between layers 1-Q.

The field amplitudes then are determined by specifying conditions for the last and first layers. In the last layer the field radiates outward so that $B_{Q+1} = 0$. In the first layer the line source imposes $A_1 = 1/\gamma_1$. These conditions combined to the global transfer relation Eq. (15) yield $A_{Q+1} = 1/\gamma_1 S_{11}(1,Q)$. All other amplitudes are then deduced from the general transfer property Eq. (13).

The matrix formulation outlined earlier is of great simplicity and computational efficiency. However, some care must be exercised in applying this method. Indeed, a problem is encountered when a particular layer L strongly attenuates the propagating waves. This is the case when $Re[\gamma_L d_L] \geq \beta$ where β is a maximum permissible attenuation (the value of β is chosen to avoid underflow or overflow problems in the numerical evaluation of the transformed field, for instance, $\beta = 6.908$ for a 60 dB attenuation).

Now, if this inequality is verified, we know that the layer completely attenuates the outgoing wave and there is no back reflected wave in the layer L: $B_L = B_{L+1} = \ldots B_{Q+1} = 0$ and $A_{L+1} = \ldots A_{Q+1} = 0$.

Under these circumstances the amplitude A_L is determined as explained earlier in the case of A_{Q+1} but now $A_L = 1/\gamma_1 S_{11}(1, L-1)$ where $S_{11}(1, L-1)$ represents the first element of the cumulated transfer matrix for layers 1-$L-1$: $S(1, L-1) = T_1 T_2 \ldots T_{L-1}$. A similar treatment may be used when attenuation occurs cumulatively over more than one layer.

It is worth noting that the previous considerations are essential to a successful numerical calculation. Indeed, a straightforward application of Eq. (15) leads in most cases to underflow or overflow diagnostics corresponding to extremely small or large exponentials in the transfer matrices T_j or in their cumulated products. These problems are avoided by first detecting such events and applying the modifications just outlined.

III. Discretization and Practical Considerations

As shown previously, the transformed pressure field $\tilde{p}(\alpha,z)$ may be obtained easily by simple matrix manipulations. It is then necessary to evaluate the Fourier transforms of $\tilde{p}(\alpha,z)$ to get $p(x,z)$.

$$p_j(x,z) = \int_{-\infty}^{+\infty} [A_j(\alpha)e^{-\gamma_j(z-z_j)} + B_j(\alpha)e^{\gamma_j(z-z_j)}]e^{i\alpha x}d\alpha \tag{16}$$

Clearly, this calculation must be performed numerically and it is most naturally done with the FFT algorithm. It is convenient first to introduce a set of reduced variables and wavenumbers: $x_* = x/\ell, z_* = z/\ell, z_{j*} = z_j/\ell, k_{j*} = k_j\ell$, $\alpha_* = \alpha\ell$, where ℓ designates the spatial extent of the computational domain. This change of variables does not alter the form of Eq. (16) so that the asterisk may be omitted in the subsequent analysis.

Now let N designate the size (the number of points) of the fast Fourier transform used in place of the continuous integral Eq. (16). Then the spatial sampling period (in the reduced set of coordinates is $\Delta x = 1/N$ and the spatial frequency period $\Delta\alpha$ is determined from the standard rule $\Delta x \Delta\alpha = 2\pi/N$. Consequently, $\Delta\alpha = 2\pi$, the spatial sampling frequency is $\alpha_S = 2\pi N$ and the maximum spatial frequency $\alpha_M = 2\pi(N/2)$. An estimate of the pressure field is then obtained from

$$\hat{p}_j(x_n,z) = \Delta\alpha \sum_{m=0}^{N-1} \tilde{p}_j(\alpha_m,z)e^{i2\pi mn/N} \tag{17}$$

where

$$x_n = n\Delta x \quad \text{for } n = 0 \ldots N/2$$
$$= -(N-n)\Delta x \quad \text{for } n = N/2+1 \ldots N-1$$

and

$$\alpha_m = m\Delta\alpha \quad \text{for } m = 0 \ldots N/2$$
$$= -(N-m)\Delta\alpha \quad \text{for } m = N/2+1 \ldots N-1$$

Under certain conditions (see, for example, Brigham[20]) this estimate constitutes a good approximation of the exact field. The main errors introduced by the discrete Fourier transform are those related to 1) the finite sampling window and 2) the discrete sampling of the spatial Fourier transform $\tilde{p}_j$. These sources of error may be reduced by augmenting the number of points of the Fourier transform. Detailed analysis of accuracy and numerical test cases show that $N = 2048$ is a suitable size in most cases.

Now it is well known that computation time of the FFT increases as $N\log_2 N$ so that much larger values of N ($\simeq 32{,}768$) may be selected to treat specific cases with a higher degree of accuracy. Further practical details may be found in Refs. 4 and 5.

IV. Source Radiation in Subsonic Shear Flows

Among all the calculations performed we selected a few typical cases of general interest. In all cases the sound speed was kept constant and with only one exception, the reduced wavenumber was set equal to 100.5 (2π) (i.e., the computation domain extended over 100.5 wavelengths). All calculations were carried with a 2048 point FFT.

In the following discussion we shall use a conventional Strouhal number $St = f\delta/U_1$ where f and δ designate the

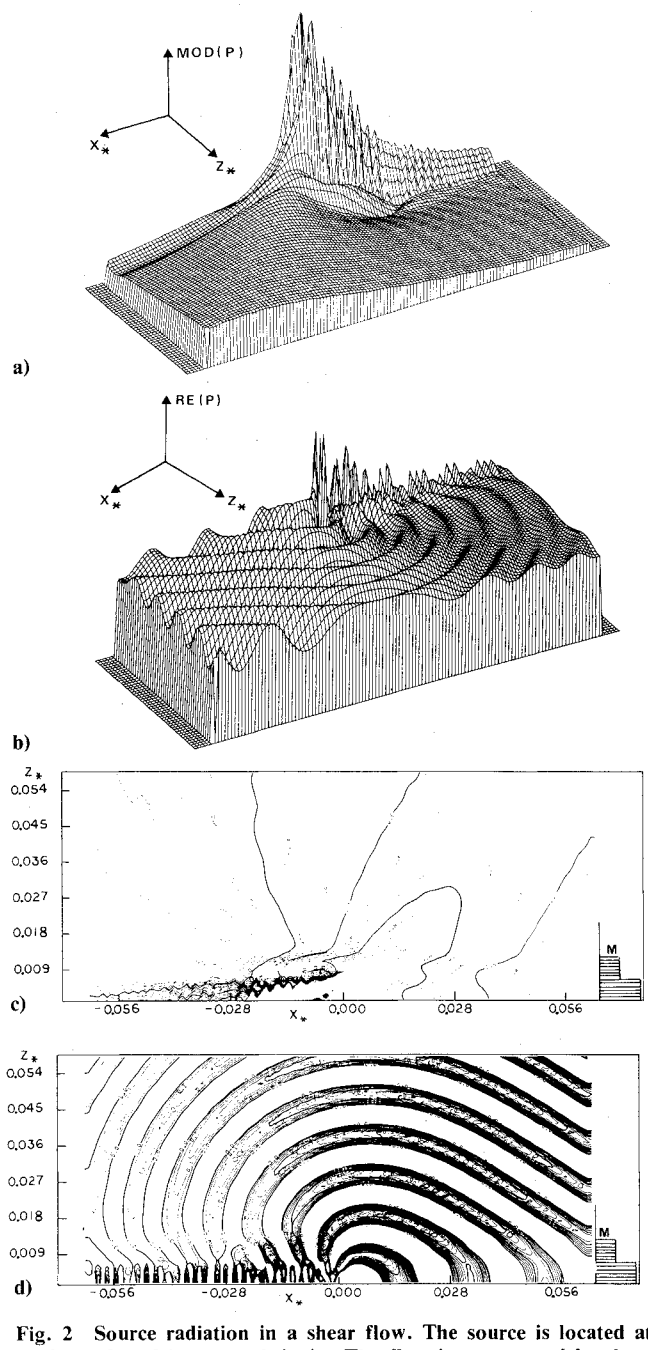

Fig. 2 Source radiation in a shear flow. The source is located at $x=0$, $z=0$ and its strength is 4π. The flow is represented by three layers: $M_1=0.8$ for $0<z\leq 0.0067$, $M_2=0.4$ for $0.0067<z\leq 0.0128$, $M_3=0$ for $0.0128<z$. Reduced wavenumber in all layers $k\ell=100.5$ (2π). a) and c) Contour plot and transection of field modulus (21 contours plotted on the [0,1] interval), b) and d) contour plot and transection of field real part (21 contours plotted on the [0,1] interval).

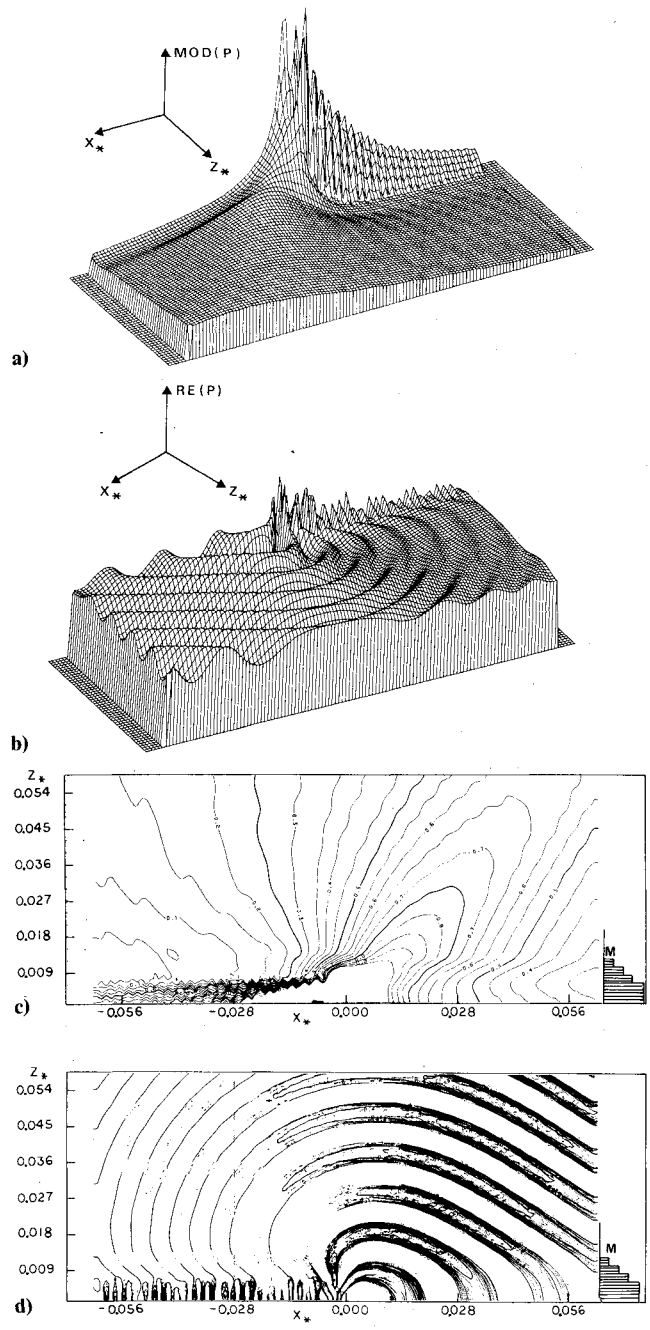

Fig. 3 Source radiation in a shear flow. The source is located at $x=0$, $z=0$ and its strength is 4π. The flow is represented by five layers: $M_1=0.8$ for $0<z\leq 0.00067$, $M_2=0.6$ for $0.0067<z\leq 0.0087$, $M_3=0.4$ for $0.0087<z\leq 0.0107$, $M_4=0.2$ for $0.0107<z\leq 0.0128$, $M_5=0$ for $0.0128<z$. Reduced wavenumber in all layers $k\ell=100.5$ (2π). a) and c) Contour plot and transection of field modulus, b) and d) contour plot and transection of field real part.

frequency and transverse extent of the shear flow. This number may be obtained from $St=k\ell\delta_*/(M_1 2\pi)$.

The first calculation (Fig. 2) corresponds to a shear flow represented by three layers. The Mach number decreases monotonically from 0.8 at the source to 0 in the outer region. The transverse dimension of the flow is $\delta_*=0.0128$ and the Strouhal number $St=1.61$. Convection and refraction clearly are important. Wavefronts are convected downstream (Fig. 2d). A reflected wave is formed upstream, inside the flow and it interferes with the direct wave. The reflected wave is much weaker downstream. In the third (semi-infinite) layer a transmitted wave is formed. The wavefronts are ovalized. They are nearly plane and parallel in the forward arc and propagate along the shear layer boundary with the phase velocity imposed by the convecting fronts inside the flow.

The radiation pattern of the source is strongly modified by the flow. It has a maximum downstream about $\Theta\simeq 50$ deg, near the direction $\cos^{-1}(1/1+M_1)$. At lower angles of propagation the plane waves forming the spatial wave spectrum are partially damped in the shear region and, as a consequence, the field modulus is reduced in the near arc. All these features are in agreement with a geometrical (high-frequency) description of the radiation process.

The second calculation (Fig. 3) corresponds to the same basic configuration but the flow is now represented by five layers instead of three and the transition between the source and the outer region is thus more gradual. The wavefield structure strongly resembles that of the previous case. The main difference is observed upstream in the vicinity of the source. This calculation clearly shows that the details of the

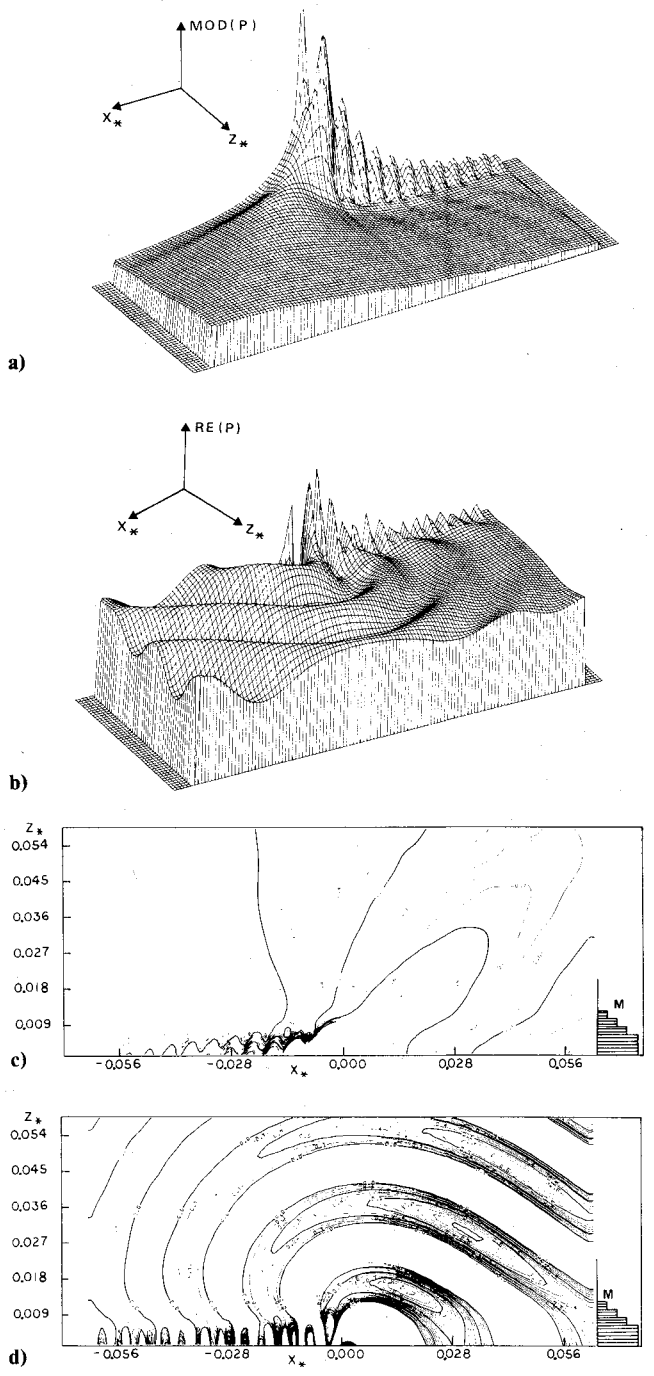

Fig. 4 Source radiation in a shear flow. Same configuration as that of Fig. 3 but the reduced wavenumber is now $k\ell = 50.5\ (2\pi)$ and the source strength has been divided by $(100.5/50.5)^{1/2}$ to allow a direct comparison with Fig. 3.

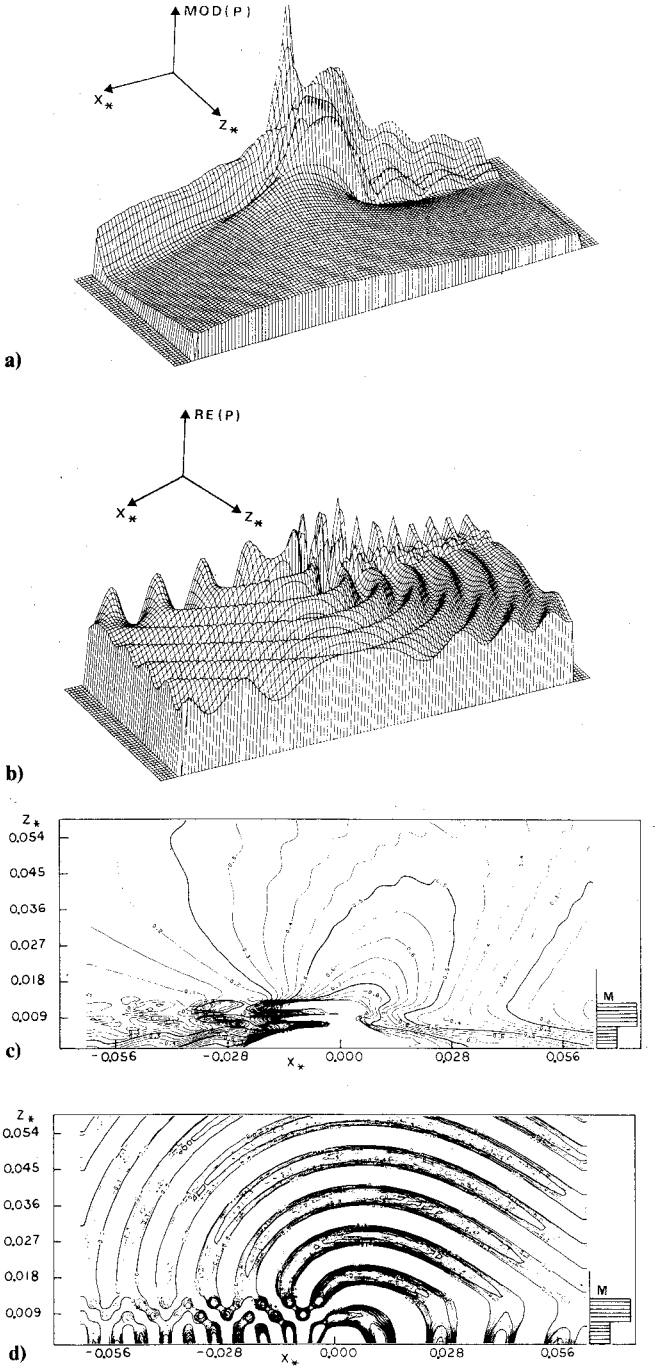

Fig. 5 Source radiation in a shear flow. Same configuration as that of Fig. 2 but the Mach number profile is inverted: $M_1 = 0.4$ for $0 < z \leq 0.0067$, $M_2 = 0.8$ for $0.0067 < z \leq 0.0128$, $M_3 = 0$ for $0.0128 < z$.

mean flow (small changes occurring on a typical scale smaller than the wavelength) only slightly influence the radiation process. This provides an a posteriori justification of the staircase representation of continuous profiles.

Another important question is that of frequency dependence of the radiation pattern. This is considered in the third calculation (Fig. 4). The flow configuration is that of the previous case but the reduced wavenumber has been cut by half, $k\ell = 50.5(2\pi)$. In these circumstances $St = 0.80$. To allow direct comparison with the previous results, the source strength has been divided by $(100.5/50.5)^{1/2}$. This ensures an exact similarity of the fields radiated by a line source operating at reduced wavenumbers of $100.5(2\pi)$ and $50.5(2\pi)$ in a medium at rest. The wavefield has the same global structure as in the previous two cases. However, the maximum values of the field modulus are displaced toward the flow axis around $\Theta \simeq 44$ deg. Contour lines in this region do not coincide with those of Figs. 2 and 3 and it is found that sound radiation actually is enhanced. The field modulus also is increased downstream while little changes occur upstream (compare Figs. 3c and 4c).

The final subsonic configuration is characterized by an inverted Mach number profile. Such profile shapes have been proposed to reduce jet noise from aircraft engines but very little analysis is available of their influence on the radiated sound field. The present calculation performed for a Strouhal

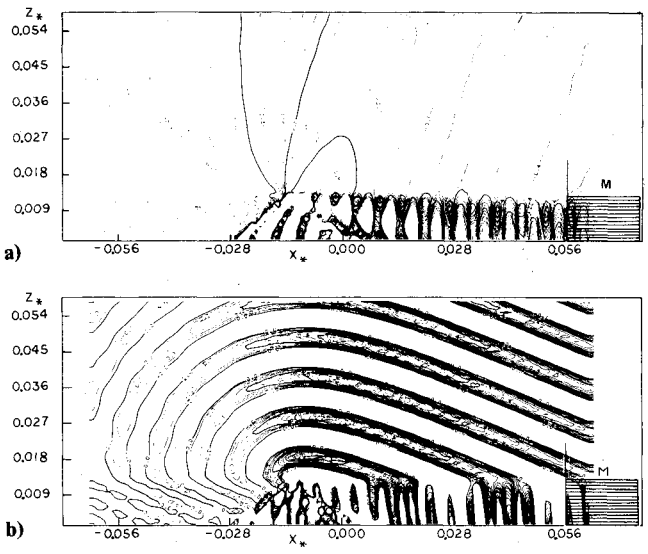

Fig. 6 Source radiation in a shear flow. The source is located at $x=-0.028$, $z=0$ and its strength is 4π. The flow in the first layer is supersonic $M_1=1.5$ for $0<z\leq 0.0128$, $M_2=0$ for $0.0128<z$. Reduced wavenumber $k\ell=100.5\ (2\pi)$, a) contour plot of field modulus and b) contour plot of field real part.

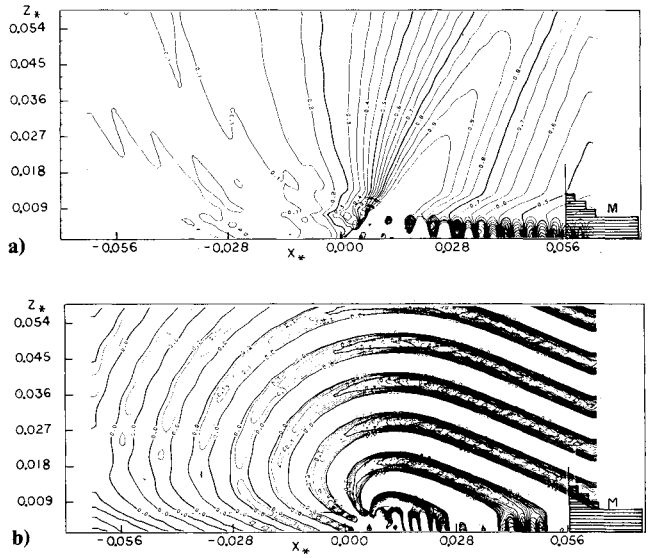

Fig. 7 Source radiation in a shear flow. The source is located at $x=0$, $z=0$ and its strength is 4π. The flow in the first layer is supersonic $M_1=1.5$ for $0<z\leq 0.0067$, $M_2=0.6$ for $0.0067<z\leq 0.0087$, $M_3=0.4$ for $0.0087<z\leq 0.0107$, $M_4=0.2$ for $0.0107<z\leq 0.0128$, $M_5=0$ for $0.0128<z$. Reduced wavenumber $k\ell=100.5\ (2\pi)$, a) contour plot of field modulus and b) contour plot of field real part.

number $St=f\delta/U_2=1.61$ equal to that of the first configuration shows a strong modification of the field pattern (Fig. 5). The radiation is less directional, the field maximum is displaced further away from the jet axis (around $\Theta\simeq 62$ deg), and its modulus is reduced in the downstream quadrant but increased upstream (compare Figs. 2c and 5c). A peculiar feature is observed upstream in the intermediate layer (Fig. 5d). The field exhibits alternating oblique wavefronts typical of guided wave propagation.

V. Source Radiation in Supersonic Shear Flows

We restrict the present section to a brief description of how the shear layer structure may influence sound radiated from a supersonic inner flow. Figure 6 corresponds to a single shear discontinuity configuration. Below this discontinuity the Mach number is $M_1=1.5$, and it is $M_2=0$ above. The wavefield structure already was examined in Ref. 5. Its most salient feature is the existence of a triangular region formed by characteristic lines originating from the source and reflected by the shear layer where the field is dominated by the direct wave (this region is apparent on Fig. 6a). Downstream of the reflected characteristic the direct and reflected waves combine and interfere in a special way. A strongly directional beam is formed in the outer region.

Now when the single shear discontinuity is replaced by a gradual subsonic transition to zero Mach number (Fig. 7) the general field structure is conserved but the transmitted field becomes more directive and its values are notably enhanced (compare Figs. 6a and 7a).

VI. Conclusion

The numerical method presented in this paper allows detailed description of sound source radiation in shear flows. It may be used to improve our understanding of acoustic/flow interactions and is also ideally suited for inclusion in a predictive theory of jet noise.

Acknowledgments

This research was performed for the main part at the Joint Institute of Aeronautics and Acoustics, Stanford University, during a summer visit authorized by ONERA and made possible by a kind invitation issued by Prof. Karamcheti. Helpful discussions with Profs. Karamcheti and Levine are gratefully acknowledged. Comments made by the reviewers have been appreciated.

References

[1] Candel, S. M., "Numerical Solution of Conservation Equations Arising in Linear Wave Theory. Application to Aeroacoustics," *Journal of Fluid Mechanics,* Vol. 83, Dec. 1977, pp. 465-493.

[2] Candel, S. M., "Etudes théoriques et expérimentales de la propagation acoustique en milieu inhomogene et en mouvement," These de Doctorat es Sciences, University of Paris VI, 1977; also, ONERA Pub. 1977-1, 1977.

[3] Candel, S. M., "Numerical Solution of Wave Scattering Problems in the Parabolic Approximation," *Journal of Fluid Mechanics,* Vol. 90, Feb. 1979, pp. 465-507.

[4] Candel, S. M. and Crance, C., "Direct Fourier Synthesis of Waves in Layered Media and the Method of the Stationary Phase," *Journal of Sound and Vibration,* Vol. 74, Feb. 1981, pp. 477-498.

[5] Candel, S. M. and Crance, C., "Direct Fourier Synthesis of Waves: Application to Acoustic Source Radiation," *AIAA Journal,* Vol. 19, March 1981, pp. 290-295.

[6] Gottlieb, P., "Sound Source Near a Velocity Discontinuity," *Journal of the Acoustical Society of America,* Vol. 32, Sept. 1960, pp. 1117-1122.

[7] Graham, E. W. and Graham, B. B., "Effect of a Shear Layer on Plane Waves of Sound in a Fluid," *Journal of the Acoustical Society of America,* Vol. 46, July 1969, pp. 169-175.

[8] Tester, B. J. and Burrin, R. H., "On Sound Radiation from Sources in Parallel Sheared Jet Flows," AIAA Paper 74-57, 1974.

[9] Goldstein, M. E., "The Low Frequency Sound from Multipole Sources in Axisymmetric Shear Flows with Application to Jet Noise," *Journal of Fluid Mechanics,* Vol. 70, Aug. 1975, pp. 595-604.

[10] Goldstein, M. E., *Aeroacoustics,* McGraw Hill, New York, 1976.

[11] Scott, J. N., "Propagation of Sound Waves Through a Linear Shear Layer," *AIAA Journal,* Vol. 17, March 1979, pp. 237-244.

[12] Koutsoyannis, S. P., Karamcheti, K., and Galant, D. C., "Acoustic Resonances and Sound Scattering by a Shear Layer," *AIAA Journal,* Vol. 18, Dec. 1980, pp. 1446-1454.

[13] Schubert, L. K., "Numerical Study of Sound Radiation by a Jet Flow I. Ray Acoustics," *Journal of the Acoustical Society of America,* Vol. 51, Feb. 1972, pp. 439-446.

[14] Ffowcs-Williams, J. E., "Sound Production at the Edge of Steady Flow," *Journal of Fluid Mechanics,* Vol. 66, Dec. 1974, pp. 791-816.

[15] Howe, M. S., "Application of Energy Conservation to the Solution of Radiation Problems Involving Uniformly Convected Source Distributions," *Journal of Sound and Vibration,* Vol. 43, Nov. 1975, pp. 77-86.

[16] Mani, R., "The Influence of Jet Flow on Jet Noise—Part 1. The Noise of Unheated Jets," *Journal of Fluid Mechanics,* Vol. 73, April 1976, pp. 753-778.

[17] Liu, C. H. and Maestrello, L., "Propagation of Sound Through a Real Jet Flowfield," *AIAA Journal,* Vol. 13, Jan. 1975, pp. 66-70.

[18] Miles, J. W., "On the Reflection of Sound at an Interface of Relative Motion," *Journal of the Acoustical Society of America,* Vol. 29, Feb. 1957, pp. 226-228.

[19] Ribner, H. S., "Reflection, Transmission, and Amplification of Sound by a Moving Medium," *Journal of the Acoustical Society of America,* Vol. 29, April 1957, pp. 435-441.

[20] Brigham, E. O., *The Fast Fourier Transform,* Prentice Hall, Englewood Cliffs, N. J., 1974.